Title

Hyperandrogenemia Induced by Letrozole Treatment of Pubertal Female Mice Results in Hyperinsulinemia Prior to Weight Gain and Insulin Resistance

Journal

Endocrinology, 158(9)

ISSN

0013-7227

Authors

Skarra, Danalea V

Hernández-Carretero, Angelina

Rivera, Alissa J

et al.

Publication Date

2017-09-01

DOI

10.1210/en.2016-1898

Hyperandrogenemia Induced by Letrozole Treatment of Pubertal Female Mice Results in Hyperinsulinemia Prior to Weight Gain and Insulin Resistance

Danalea V. Skarra,[1]* Angelina Hernández-Carretero,[2]* Alissa J. Rivera,[1] Arya R. Anvar,[1] and Varykina G. Thackray[1]

[1]Department of Reproductive Medicine, University of California, San Diego, La Jolla, California 92093; and [2]Department of Medicine, University of California, San Diego, La Jolla, California 92093

Women with polycystic ovary syndrome (PCOS) diagnosed with hyperandrogenism and ovulatory dysfunction have an increased risk of developing metabolic disorders, including type 2 diabetes and cardiovascular disease. We previously developed a model that uses letrozole to elevate endogenous testosterone levels in female mice. This model has hallmarks of PCOS, including hyperandrogenism, anovulation, and polycystic ovaries, as well as increased abdominal adiposity and glucose intolerance. In the current study, we further characterized the metabolic dysfunction that occurs after letrozole treatment to determine whether this model represents a PCOS-like metabolic phenotype. We focused on whether letrozole treatment results in altered pancreatic or liver function as well as insulin resistance. We also investigated whether hyperinsulinemia occurs secondary to weight gain and insulin resistance in this model or if it can occur independently. Our study demonstrated that letrozole-treated mice developed hyperinsulinemia after 1 week of treatment and without evidence of insulin resistance. After 2 weeks of letrozole treatment, mice became significantly heavier than placebo mice, demonstrating that weight gain was not required to develop hyperinsulinemia. After 5 weeks of letrozole treatment, mice exhibited blunted glucose-stimulated insulin secretion, insulin resistance, and impaired insulin-induced phosphorylation of AKT in skeletal muscle. Moreover, letrozole-treated mice exhibited dyslipidemia after 5 weeks of treatment but no evidence of hepatic disease. Our study demonstrated that the letrozole-induced PCOS mouse model exhibits multiple features of the metabolic dysregulation observed in obese, hyperandrogenic women with PCOS. This model will be useful for mechanistic studies investigating how hyperandrogenemia affects metabolism in females. (***Endocrinology*** **158: 2988–3003, 2017)**

Polycystic ovary syndrome (PCOS) is the most common endocrine disorder in women of reproductive age and has an estimated worldwide prevalence of 6% to 15% using the National Institutes of Health diagnostic criteria and up to 21% using the Rotterdam Consensus criteria (1, 2). Women with PCOS have an increased risk of menstrual irregularities, infertility, and pregnancy complications (1, 3, 4). PCOS was first described in 1935 by Irving Stein and Michael Leventhal as a triad of polycystic ovaries, hirsutism and oligomenorrhea or amenorrhea (5, 6). Over 80 years later, PCOS is still diagnosed using variations of these clinical hallmarks. For instance, the National Institutes of Health 1990 PCOS diagnostic criteria consists of clinical hyperandrogenism and oligomenorrhea or amenorrhea, whereas the Rotterdam Consensus 2003 criteria require at least two of the three criteria (hyperandrogenism, oligomenorrhea or amenorrhea, and polycystic ovaries),

ISSN Print 0013-7227 ISSN Online 1945-7170
Printed in USA

Received 5 December 2016. Accepted 11 July 2017.
First Published Online 14 July 2017

*These authors contributed equally to this study.

Abbreviations: ALT, alanine aminotransferase; AR, androgen receptor; AST, aspartate aminotransferase; DHEA, dehydroepiandrosterone; DHT, dihydrotestosterone; ELISA, enzyme-linked immunosorbent assay; FBG, fasting blood glucose; GSIS, glucose-stimulated insulin secretion; GTT, glucose tolerance test; HDL, high-density lipoprotein; IL-6, interleukin 6; ITT, insulin tolerance test; LH, luteinizing hormone; NAFLD, nonalcoholic fatty liver disease; PCOS, polycystic ovary syndrome; PND, postnatal day; RRID, Research Resource Identifier; SAB, secretion assay buffer; VCO_2, CO_2 production; VO_2, O_2 consumption.

and the Androgen Excess Society 2006 criteria include hyperandrogenism and ovulatory dysfunction (1).

Although PCOS was originally described as a reproductive disorder, studies over the past 30 years have demonstrated that PCOS is also a metabolic disorder (7–12). In their seminal study, Stein and Leventhal (6) identified an association between PCOS and obesity, and epidemiology studies have shown that approximately 80% of women diagnosed with PCOS in the United States are overweight or obese (4). Although not a diagnostic criterion, insulin resistance is also prevalent in women with PCOS, occurring in 75% of nonobese and 95% of obese women with PCOS (13). In addition to obesity and insulin resistance, clinical studies have shown that PCOS is associated with abdominal adiposity, hyperinsulinemia, glucose intolerance, and dyslipidemia (14–17).

Due to metabolic dysregulation, women with PCOS have an increased risk of developing metabolic syndrome, type 2 diabetes, gestational diabetes, nonalcoholic fatty liver disease (NAFLD), and cardiovascular disease (3, 12, 18–20). A large, retrospective study demonstrated that PCOS was associated with an increased risk of obesity (16% vs 3.7%), type 2 diabetes (12.5% vs 3.8%), and hypertensive disorder (3.8% vs 0.7%) over a 15-year period (21). Similarly, a meta-analysis of 35 studies found that PCOS was associated with a fourfold increase in the prevalence of type 2 diabetes (22). There is strong evidence that hyperandrogenism is the primary predictor of metabolic dysfunction (2, 4, 12). Metabolic dysfunction occurs predominantly in women with PCOS who are diagnosed with hyperandrogenism and ovulatory dysfunction, irrespective of body mass index (2, 23, 24). This association is weaker for women with hyperandrogenism and polycystic ovaries, whereas women with ovulatory dysfunction and polycystic ovaries, but no evidence of androgen excess, have the mildest degree of metabolic dysfunction.

Although the etiology of PCOS is poorly understood, heritability and twin studies indicate that there is a strong genetic component, whereas environmental factors such as prenatal exposure to androgens may also play a role (25–30). Because hyperandrogenism is associated with both reproductive and metabolic phenotypes of PCOS, researchers have created models in primates, sheep, and rodents to study the role of androgens in the development and pathology of PCOS [reviewed in (31–35)]. There are many advantages to using mice as a model system, including a short generation time, amenability to genetic manipulation, and the ability to control genetics and diet. Several hyperandrogenic mouse models have been developed using dihydrotestosterone (DHT) or dehydroepiandrosterone (DHEA), but none of these models fully recapitulated the reproductive and metabolic phenotypes of PCOS. For instance, prenatal exposure to DHT was reported in several studies to result in disrupted estrous cyclicity but not polycystic ovaries or a consistent metabolic phenotype (36–39). In comparison, pubertal treatment with DHT resulted in disrupted cyclicity, polycystic ovaries, weight gain, adipocyte hypertrophy, and glucose intolerance but did not result in increased luteinizing hormone (LH) levels, hyperinsulinemia, hyperglycemia, or insulin resistance (40). Pubertal treatment with DHEA resulted in acyclicity and hyperinsulinemia but no polycystic ovaries, weight gain, or hyperglycemia (41). Another study, using 10-fold less DHEA, resulted in a stronger metabolic phenotype, including weight gain, hyperglycemia, and hyperinsulinemia, but still lacked polycystic ovaries (42).

We previously developed a mouse model that uses letrozole, a nonsteroidal aromatase inhibitor, to increase endogenous testosterone levels by limiting the conversion of testosterone to estrogen (43). We demonstrated that this mouse model has many of the hallmarks of PCOS, including hyperandrogenism, elevated LH levels, anovulation, and polycystic ovaries (43, 44). In addition, we reported that these mice have a metabolic phenotype that includes increased weight and fat mass, visceral adiposity, adipocyte hypertrophy, and impaired glucose tolerance after 5 weeks of letrozole treatment (43, 44). In this study, we investigated whether letrozole treatment results in altered pancreatic or liver function as well as insulin resistance. We also asked whether hyperinsulinemia occurs as a consequence of weight gain and insulin resistance in this model or if it can occur independently. In addition to demonstrating that many of the metabolic features of this model are consistent with those found in obese women with PCOS, our study shows that hyperinsulinemia and mild dysglycemia occur prior to weight gain and the development of insulin resistance in letrozole-treated female mice. In addition, our data indicate that letrozole treatment may result in tissue-specific insulin resistance, as demonstrated by decreased insulin-dependent phosphorylation of AKT within skeletal muscle.

Materials and Methods

Animals

Female C57BL/6NHsd mice were purchased from Envigo at 3 weeks of age and allowed to acclimate for 1 week prior to initiating studies. Mice were housed under automated 12/12-hour light/dark (light period: 0600 to 1800 hours) and given *ad libitum* access to water and food (Teklad S-2335 diet; Envigo). All animal studies were approved by the University of California, San Diego Institutional and Animal Care and Use Committee (protocol number S14011). At 4 weeks of age, mice

were implanted subcutaneously with either a placebo or letrozole (Fitzgerald Industries International) pellet in the nape that provided a constant, slow release of letrozole (3-mg pellet 3 mm in diameter, 50 μg/d release; Innovative Research of America). Each week, mice were weighed and then fasted for 6 hours, starting at 0900 hours, to obtain tail vein blood to measure fasting blood glucose (FBG) and/or insulin. Food intake was also measured on a weekly basis.

Metabolic and locomotor analyses

Indirect calorimetry was performed on a separate cohort of female mice treated with placebo or letrozole for 5 weeks using a 12-cage equal-flow Comprehensive Lab Animal Monitoring System calorimeter (Columbus Instruments) coupled with photosensors to detect movement. The mice were habituated to the metabolic cages (single-housed) for 2 days prior to data acquisition for 3 days (n = 6 per group). O_2 consumption (VO_2) and CO_2 production (VCO_2) were measured every 12 minutes per cage. Respiratory exchange ratio was calculated as the quotient of VCO_2/VO_2 . Locomotor activity was measured at 1-minute intervals by photosensors, with the bottom row measuring horizontal movement (equals the total number of photobeams broken; nonrepetitive activity equals total horizontal movement minus the number of consecutive beams broken due to nonambulatory movements like grooming) and the upper row measuring vertical movement (rearing, reaching the drinking tube, walking on top of the food hopper). Total activity equals horizontal plus vertical movement. In addition, food and water intake was measured at 12-minute intervals.

In vivo glucose-stimulated insulin secretion

A glucose tolerance test (GTT) was performed on mice after 1 week and 5 weeks of placebo or letrozole treatment. The mice were fasted for 6 hours (0900 to 1500 hours). Tail vein blood was collected and glucose levels were measured using a handheld glucometer (One Touch UltraMini; LifeScan) just before (time 0) an intraperitoneal injection of glucose was administered (2 g/kg body weight in sterile saline) and at 15, 30, 45, 60, 90, and 120 minutes after injection. To measure glucose-stimulated insulin secretion (GSIS), additional tail vein blood was collected at 0, 3, 10, and 30 minutes.

Ex vivo GSIS

Islets were isolated by inflating the pancreas via the common bile duct with 3 mL of reconstituted CIzyme RI (VitaCyte, LLC) per the manufacturer's instructions. Pancreata were digested at 37°C for 17 minutes, and islets were separated using a gradient of Histopaque 1119:1077 (Sigma) at a 1.2:1 ratio layered over 0.3% bovine serum albumin–containing Hanks balanced salt solution. Islets were selected and incubated for 48 hours in Dulbecco's modified Eagle medium containing 1 g/L glucose, 10% fetal bovine serum, 50 U/mL penicillin and streptomycin, and either ethanol vehicle or 10 nM DHT. *Ex vivo* GSIS was performed as previously described (45) with some modifications. Islets were incubated with either ethanol vehicle or DHT throughout the entire protocol. Thirteen size-matched islets were preincubated for 70 minutes in 2.8 mM glucose in secretion assay buffer (SAB) (0.114 M NaCl, 4.7 mM KCl, 1.2 mM KH_2PO_4, 1.16 mM $MgSO_4$) with 1 M HEPES, 0.25 M $CaCl_2$, 35% bovine serum albumin (0.2%), and 25.5 mM $NaHCO_3$. Islets were then switched to fresh 2.8-mM glucose-containing SAB buffer for 1 hour, and media were collected to measure basal levels of secreted insulin. The islets were subsequently incubated in 16.7 mM glucose-containing SAB buffer for 1 hour, and media were collected to measure stimulated levels of secreted insulin. Islets were then washed and lysed in acidic ethanol (80% ethanol, 2.1% 12N HCl) and diluted 1:25 in SAB to obtain total intracellular insulin content. Each sample was run in duplicate to measure insulin levels with an enzyme-linked immunosorbent assay (ELISA) ultrasensitive or high-range kit (ALPCO).

Insulin tolerance test

In a separate cohort of mice, an insulin tolerance test (ITT) was performed on mice after 1 week and 5 weeks of placebo or letrozole treatment. Mice were fasted for 5 hours (0900 to 1400 hours) (46). Tail vein blood glucose was measured just before (time 0) an intraperitoneal injection of insulin (0.75 U/kg in sterile saline; Humulin R U-100; Eli Lilly) was given and at 15, 30, 45, 60, 90, and 120 minutes after injection.

Ex vivo insulin challenge and Western blots

Mice were fasted for 5 hours (0900 to 1400 hours) and then placed under isofluorane anesthesia. Tissue samples were collected from liver, parametrial adipose, and quadricep skeletal muscle just prior to insulin injection. Insulin (1.5 U/kg in sterile saline) was then injected into the inferior vena cava (47). Tissues were collected as follows after injection: liver at 3 minutes, skeletal at 7 minutes, and adipose at 10 minutes and then snap frozen in liquid nitrogen. Liver and skeletal muscle samples were homogenized in ice-cold radioimmunoprecipitation assay buffer [10 mM Tris-HCl (pH 7.4), 150 mM NaCl, 1% Triton X-100, 1 mM EDTA, 0.1% sodium dodecyl sulfate, 1% sodium deoxycholate, 1 mM phenylmethylsulfonyl fluoride, complete protease inhibitor tablet and phosphatase inhibitor tablet (Roche Applied Science)] and adipose in ice-cold HNTG buffer [50 mM HEPES (pH 7.5), 150 mM NaCl, 0.1% Triton X-100, 10% glycerol, complete protease inhibitor tablet and phosphatase inhibitor tablet (Roche Applied Science), 1 mM phenylmethylsulfonyl fluoride] using a Bio-Gen Pro200 Homogenizer (Pro Scientific). Lysates were centrifuged at 16,000 × *g* at 4°C for 30 minutes. For adipose samples, the fat cakes were removed from the supernatant. The protein concentration of the supernatant was determined by Bradford assay (Bio-Rad Laboratories), and an equal amount of protein per sample was loaded onto a 10% sodium dodecyl sulfate–polyacrylamide gel electrophoresis gel. Proteins were resolved by electrophoresis and transferred for 2 hours at 100 V onto a polyvinylidene difluoride membrane (Millipore). Blots were blocked overnight in 5% nonfat milk and then probed overnight at 4°C with primary antibody. Primary antibodies used for the Western blot were AKT [1:3000; sc-8312; Research Resource Identifier (RRID): AB_671714] and glyceraldehyde 3-phosphate dehydrogenase (1:3000; sc-25778; RRID: AB_10167668) from Santa Cruz Biotechnology and phospho-AKTS473 (1:2000; 4051; RRID: AB_331158) from Cell Signaling Technology. Blots were washed and then incubated with anti-rabbit horseradish peroxidase–linked (1:5000; sc-2004; RRID: AB_631746) or anti-mouse horseradish peroxidase secondary antibody (1:3000; sc-2005; RRID: AB_631736) as appropriate (Santa Cruz Biotechnology). Bands were visualized using the SuperSignal West Dura Substrate (Thermo Scientific). Band intensity was

quantified by densitometry using ImageJ software (National Institutes of Health).

Hormone assays

Serum testosterone was measured with a mouse ELISA (range, 10 to 800 ng/dL), LH was measured with a radioimmunoassay (range, 0.04 to -75 ng/mL), and 17-β estradiol was measured with a mouse ELISA (range, 3 to 300 pg/mL) by the University of Virginia Center for Research in Reproduction Ligand Assay and Analysis Core Facility. Leptin was measured with a mouse ELISA (range, 62.5 to 4000 pg/mL; R&D Systems). Glucagon was measured with a mouse ELISA (range, 31.3 to 2000 pg/mL; R&D Systems). Serum insulin and interleukin 6 (IL-6) were measured using a Milliplex Mouse Metabolic Hormone Panel (MMHMAG-44K; Millipore) using a Luminex Magpix (range for insulin, 69 to 50,000 pg/mL; range for IL-6, 27 to 10,000 pg/mL).

Lipid and hepatic enzyme assays

The University of Texas Southwestern Medical Center Metabolic Phenotyping Core (Dallas, TX) analyzed serum free fatty acids with the WAKO Diagnostics NEFA colorimetric assay (range, 0.01 to 4 mEq/L) and serum chemistries using the Vitros 250 Chemistry System for total cholesterol (range, 50 to 326 mg/dL), triglycerides (range, 10 to 525 mg/dL), high-density lipoprotein (HDL) (range, 5 to 110 mg/dL), aspartate aminotransferase (AST; range, 14 to 373 U/L), and alanine aminotransferase (ALT; range, 15 to 644 U/L).

Histology

Liver and ovaries were collected from mice, fixed in 4% paraformaldehyde at room temperature for 16 to 24 hours, and stored in 70% ethanol before processing for histology. Paraffin-embedded ovaries were sectioned at 10 μm and liver at 7 μm, and both tissues were stained with hematoxylin and eosin (Zyagen). Digital images were collected using a Nikon Digital Shot-Fi1 camera.

Statistical analyses

Statistical analyses were conducted using JMP 12.0Pro (SAS Institute). Repeated-measure longitudinal studies were analyzed by mixed-effects model analysis (48), and independent data samples were analyzed by Student *t* test or one-way analysis of variance followed by Tukey *post hoc* test. For nonnormal data, nonparametric Kruskal-Wallis analysis was used followed by the Steel-Dwass *post hoc* test. Area under the curve was calculated by the trapezoid rule.

RESULTS

Pubertal female mice gained weight after 2 weeks of letrozole treatment, but food intake and energy expenditure remained unchanged

We previously established a letrozole-induced PCOS mouse model to characterize the role of hyperandrogenemia in the reproductive and metabolic dysregulation observed in PCOS (43). We again used 5 weeks of letrozole treatment in 4- to 9-week-old female mice in the current study to further characterize the metabolic dysregulation that occurs in the PCOS mouse model [Fig. 1(a)]. As previously reported (43, 44), pubertal mice treated with letrozole for 5 weeks had multiple hallmarks of PCOS, including elevated testosterone, anovulation as indicated by a lack of corpora lutea in the ovaries, and cystic follicles (Supplemental Fig. 1). We found that mice had a significant increase in body weight after 2 weeks of letrozole treatment compared with placebo that was maintained for the rest of the experiment [Fig. 1(b)]. Interestingly, although weight significantly increased during letrozole treatment, we did not observe any change in weekly food intake during the study [Fig. 1(c)]. To further investigate the metabolic phenotype of this PCOS mouse model, we placed placebo- or letrozole-treated mice in CLAMS cages after 5 weeks of treatment. Food and water intake did not change in the light or dark cycle (Supplemental Fig. 2). Locomotor activity was significantly decreased in letrozole-treated mice during the dark cycle but not in the light cycle [Fig. 1(d); Supplemental Fig. 2]. There was also a small decrease in respiration (VO_2 and VCO_2) in letrozole-treated mice in the dark cycle, potentially due to decreased movement, although it was not statistically significant [Fig. 1(e) and 1(f)]. In contrast, letrozole treatment did not significantly alter the respiratory exchange ratio or total energy expenditure in the dark or light cycle [Fig. 1(g) and 1(h)]. These results indicate that energy intake and expenditure were not altered by letrozole treatment, even though movement and respiration were decreased and suggest that other mechanisms contribute to the metabolic dysregulation observed after letrozole treatment.

Glucose homeostasis was disrupted after 5 weeks of letrozole treatment

Previously, we reported that glucose responsiveness in a GTT was altered after 5 weeks of letrozole treatment (43, 44). Therefore, to further investigate this defect in glucose homeostasis, *in vivo* GSIS was measured along with serum glucagon levels in mice after 5 weeks of letrozole or placebo treatment. *In vivo* GSIS was performed after the mice were fasted for 6 hours [Fig. 2(a–e)]. Similar to our previous study (43, 44), mice treated with letrozole for 5 weeks had significantly elevated FBG [Fig. 2(b)]. Letrozole-treated mice also had impaired glucose tolerance over 2 hours, as previously reported [Fig. 2(a–c)] (43, 44). Interestingly, letrozole-treated mice had fasting basal insulin levels that were almost four times higher than placebo mice [Fig. 2(d)]. Both groups had peak GSIS 10 minutes after injection [Fig. 2(d)]. When normalized to basal insulin levels, placebo-treated mice responded to exogenous glucose stimulation with a maximal secretion peak 3.5-fold greater than basal insulin levels. In contrast, letrozole-treated

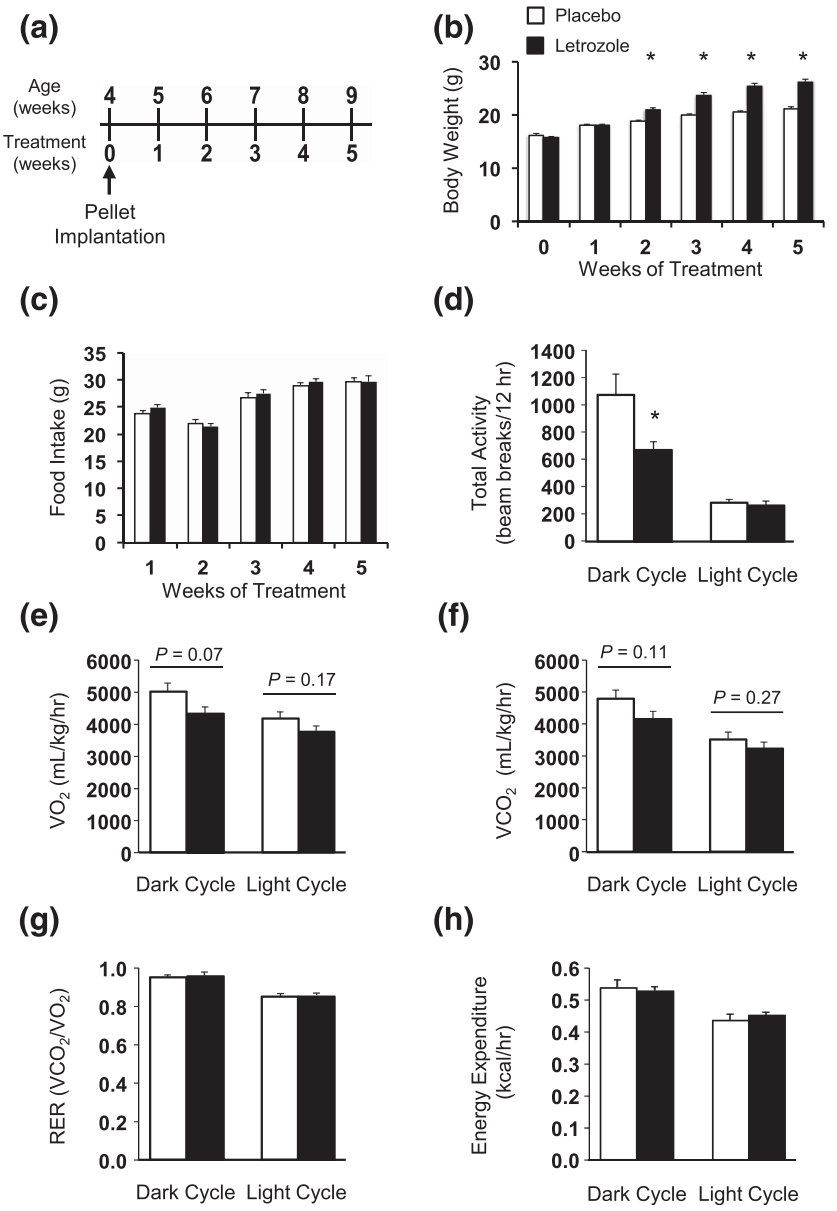

Figure 1. Body weight increased with letrozole treatment but food intake and total energy expenditure remained unchanged. (a) Schematic of placebo and letrozole treatment paradigm. Starting at 4 weeks of age, female mice were implanted with subcutaneous placebo or letrozole pellets, which provided constant dosing until the end of the experiment. (b) Mice had increased body weight after 2 weeks of treatment; n = 16 to 19 per group; $*P < 0.05$ placebo vs letrozole by mixed-effects model analysis. (c) Food intake was not different between groups over the 5-week treatment period; n = 8 per group. (d) Total locomotor activity as measured by beam breaks in CLAMS cages was decreased after 5 weeks of letrozole treatment in the dark cycle but not the light cycle; n = 6 per group. $*P < 0.05$ by *t* test. (e–h) The volume of oxygen and carbon dioxide, the RER, and total energy expenditure were not significantly altered after 5 weeks of letrozole treatment. RER, respiratory exchange ratio.

mice displayed a blunted response to glucose stimulation with a maximal peak of 1.3-fold greater than basal insulin levels [Fig. 2(e)]. This experiment suggests that letrozole treatment increases basal insulin secretion and/or, alternatively, that insulin clearance is decreased. These data also suggest that β-cells in these mice do not secrete insulin appropriately in response to exogenous glucose; however, additional studies are needed to confirm this finding.

Glucagon levels were decreased in fasted mice after 5 weeks of letrozole treatment

In the fasted state, glucagon levels are elevated to stimulate hepatic glycogenolysis and gluconeogenesis to provide a constant source of glucose. In the fed state, increased insulin suppresses both glucagon secretion and hepatic glucose production (49, 50). To determine if abnormal glucagon secretion was associated with the hyperglycemia we observed in letrozole-treated mice, we measured serum glucagon from mice after 5 weeks of letrozole treatment that were in a fasted or fed state. As expected, glucagon levels in placebo-treated mice were significantly lower in an *ad libitum* fed state compared with a fasted state [Fig. 2(f)]. Similarly, letrozole-treated mice had decreased glucagon levels in a fed state compared with a fasted state, indicating that pancreatic α-cells can secrete glucagon in response to a fast. Glucagon levels were not different between placebo and letrozole mice in the *ad libitum* fed state, suggesting that suppression of glucagon in the fed state was normal. Interestingly, we observed a modest but significant decrease in glucagon levels in fasted letrozole-treated mice compared with fasted placebo mice [Fig. 2(f)].

Glucose stimulated insulin secretion was not altered by DHT treatment in pancreatic islets isolated from placebo- or letrozole-treated female mice

To further investigate β-cell function, we performed an *ex vivo* GSIS in islets isolated from male or female mice. Islets were cultured for 48 hours in ethanol vehicle or DHT and then treated with basal levels of glucose (2.8 mM) and then further stimulated with high glucose (16.7 mM). Similar to a previous study (51), we observed an increase in GSIS in islets isolated from male mice that were treated with DHT for 48 hours compared with vehicle [Fig. 3(a)]. In contrast, we did not observe an

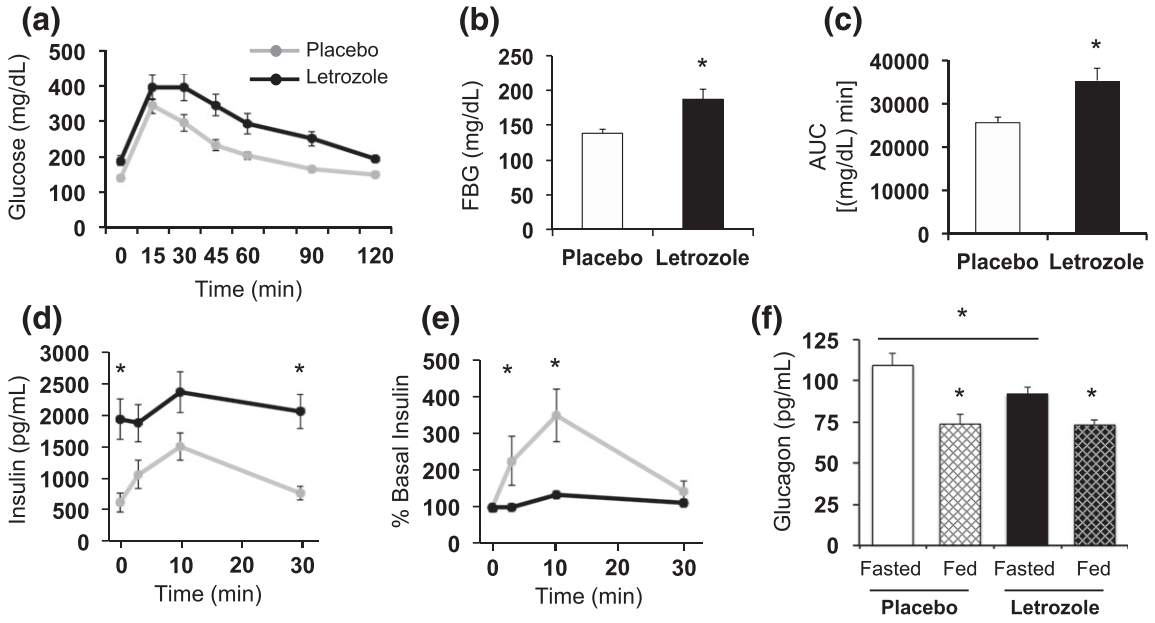

Figure 2. Glucose homeostasis was disrupted after 5 weeks of letrozole treatment. (a–e) Results from an *in vivo* GSIS test; n = 6 per group. (a) Impaired glucose tolerance was observed in letrozole-treated mice. (b) FBG was increased in letrozole-treated mice; $*P < 0.05$ by *t* test. (c) Blood glucose area under the curve (AUC) was increased in letrozole-treated mice; $*P < 0.05$ by *t* test. (d) Serum insulin levels during GSIS and (e) percent relative to basal insulin demonstrated that letrozole-treated mice had a blunted insulin secretion response to glucose stimulation; $*P < 0.05$ placebo vs letrozole by mixed-effects model analysis. (f) Serum glucagon levels were measured after a 6-hour fast (Fasted; n = 8 to 12 per group) or after *ad libitum* feeding (Fed; n = 7 to 8 per group); $*P < 0.05$ fasted vs fed or fasted placebo vs letrozole by mixed-effects model analysis.

increase in GSIS in islets from female mice treated with DHT, indicating that there was a sex-specific response to DHT [Fig. 3(a)]. We then investigated whether GSIS is altered in islets from placebo- and letrozole-treated mice after 5 weeks of treatment. Both basal- and high glucose–stimulated insulin secretion were similar between islets from placebo- and letrozole-treated mice [Fig. 3(b)], suggesting that a direct effect of DHT on insulin secretion is not responsible for the hyperinsulinemia or the impaired GSIS observed in letrozole-treated mice.

Mice were insulin resistant after 5 weeks of letrozole treatment

We assessed insulin resistance in mice after 5 weeks of treatment using an ITT. Both treatment groups displayed a decrease in blood glucose in response to exogenous insulin [Fig. 4(a)]. When normalized to basal FBG, placebo-treated mice had a maximal decrease to 35% of basal glucose, whereas letrozole-treated mice only displayed a reduction to 70% of basal glucose, suggesting that letrozole treatment resulted in peripheral insulin resistance [Fig. 4(b)].

Peripheral insulin resistance can be identified in insulin target tissues, such as liver and adipose tissues, and skeletal muscle by changes within the insulin signaling pathway (52). Therefore, we performed an *ex vivo* insulin challenge to assess changes in peripheral tissue insulin sensitivity in mice after 5 weeks of treatment. Using Western blotting, we measured phosphorylation of AKT Serine473 as an indirect measure of insulin signaling cascade activation [Fig. 4(c) and 4(d)] (47). We found that adipose and liver phosphorylation of AKT in response to exogenous insulin relative to basal phosphorylation was similar in placebo- and letrozole-treated mice. In contrast, insulin-induced AKT phosphorylation was significantly blunted in the skeletal muscle of mice treated with letrozole, suggestive of tissue-specific insulin resistance.

Mice were hyperlipidemic after 5 weeks of letrozole treatment

We evaluated serum lipids in placebo- and letrozole-treated mice after 5 weeks of treatment. We found that letrozole treatment was associated with significantly elevated lipids, including total cholesterol, triglycerides, and free fatty acids, similar to the dyslipidemia found in many women with PCOS (Table 1) (14, 53). HDL was also elevated, which is not typically found in women with PCOS. Leptin levels were elevated in letrozole-treated mice, consistent with the increased adiposity observed in this model. A previous report identified increased inflammatory markers and macrophage infiltration in parametrial adipose tissue in mice after 5 weeks of letrozole treatment (43). In contrast, serum levels of IL-6 were similar in placebo- and letrozole-treated mice

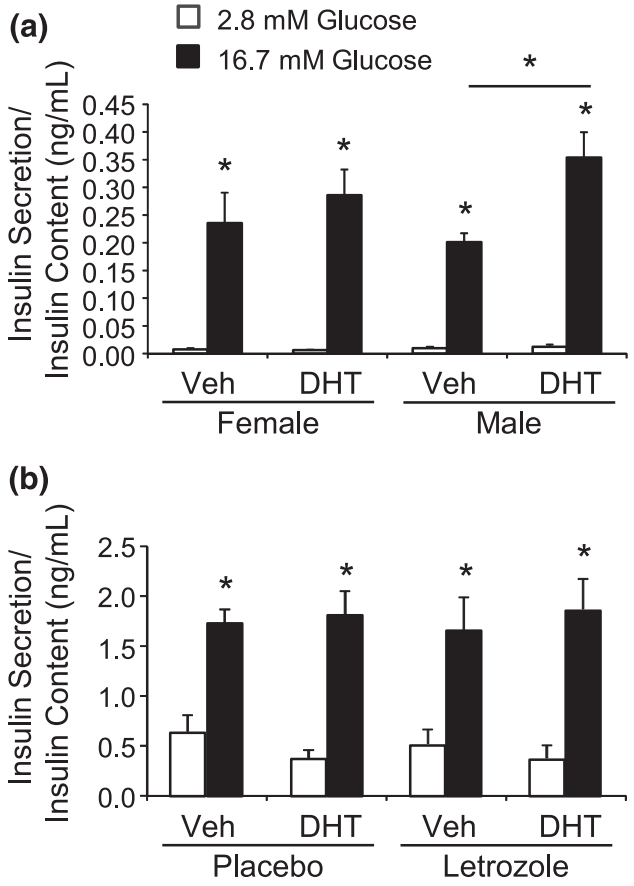

Figure 3. DHT treatment did not alter *ex vivo* glucose stimulated insulin secretion in islets isolated from placebo- or letrozole-treated female mice. (a) Islets were isolated from 8- to 10-week-old female and male mice and cultured for 48 hours with ethanol vehicle (Veh) or 10 nM DHT (n = 7 per group). GSIS was performed in static culture. Media were collected from islets treated with 2.8 mM glucose and then 16.7 mM glucose for 1 hour to measure insulin secretion. DHT treatment resulted in a significant increase in GSIS in islets isolated from male mice but not female mice. $*P < 0.05$ 2.8 mM vs 16.7 mM glucose and Veh vs DHT-treated male mice by nonparametric Kruskal-Wallis analysis followed by Steel-Dwass *post hoc* test. (b) Islets were isolated from placebo- or letrozole-treated mice after 5 weeks of treatment and cultured for 48 hours with Veh or 10 nM DHT (n = 7 per group). Media were collected from islets treated with 2.8 mM glucose and then 16.7 mM glucose for 1 hour to measure insulin secretion. DHT treatment did not alter GSIS in islets isolated from placebo- or letrozole-treated female mice. $*P < 0.05$ 2.8 mM vs 16.7 mM glucose by one-way analysis of variance followed by Tukey *post hoc* test.

(Table 1), suggesting that systemic inflammation did not occur after 5 weeks of letrozole treatment.

Liver function and histology were normal after 5 weeks of letrozole treatment

Because letrozole treatment resulted in dyslipidemia in this mouse model, we assessed liver histology and serum enzymes to evaluate for possible liver disease. ALT and AST are enzymes that are released from damaged hepatocytes (20). Letrozole-treated mice had no signs of liver injury as both serum ALT and AST levels were normal [Fig. 5(a) and 5(b)]. In addition, there were no signs of ectopic lipid deposits in the livers of letrozole-treated mice [Fig. 5(c)], despite the hyperlipidemia, further indicating that liver function was unaffected after 5 weeks of letrozole treatment.

Hyperglycemia and hyperinsulinemia were present after 1 week of letrozole treatment and occurred prior to weight gain

The metabolic dysregulation that we observed in female mice after 5 weeks of letrozole treatment, including mild hyperglycemia, hyperinsulinemia, insulin resistance, and dyslipidemia, could have developed secondary to the significant increase in adiposity that occurred after 2 weeks of treatment. To determine if increased adiposity caused hyperinsulinemia and hyperglycemia in the letrozole-induced PCOS mouse model, we measured weekly FBG and insulin levels. As shown in Fig. 6, significant hyperinsulinemia and hyperglycemia occurred after 1 week of letrozole treatment (the earliest time point we measured). After 1 week of treatment, average FBG was 155 mg/dL in placebo-treated mice compared with 190 mg/dL in letrozole-treated mice [Fig. 6(a)]. FBG levels remained elevated in letrozole-treated mice during weeks 1 to 5. In addition, from week 0 to week 1 of treatment, average fasting insulin levels of placebo-treated mice increased from 633 pg/mL to 1043 pg/mL, and letrozole-treated mice levels increased from 634 pg/mL to 1482 pg/mL [Fig. 6(b)]. The increase in insulin levels in the placebo group is consistent with metabolic changes that occur during puberty, which include increased insulin resistance and a compensatory increase in insulin to maintain euglycemia (54). Puberty in female C57BL/6 mice is evident at 4 weeks of age by vaginal opening, and cyclicity is established by 8 weeks of age (55). As mice progress through puberty and into sexual maturity, insulin resistance subsides and insulin levels return to prepubertal levels, as demonstrated in the placebo-treated mice in Fig. 6(b). In contrast to placebo, letrozole treatment resulted in a significant increase in fasting insulin levels after 1 week of treatment that became more pronounced after 3 to 5 weeks of treatment [Fig. 6(b)]. Overall, these data demonstrated that letrozole treatment resulted in a rapid increase in glucose and insulin levels after 1 week of treatment and that these changes occurred prior to any measurable increase in weight.

Testosterone and LH were increased after 1 week of letrozole treatment

Because metabolic changes occurred after 1 week of letrozole treatment (at 5 weeks of age), we assessed whether letrozole treatment also resulted in changes in reproductive hormones at this time point. Similar to the

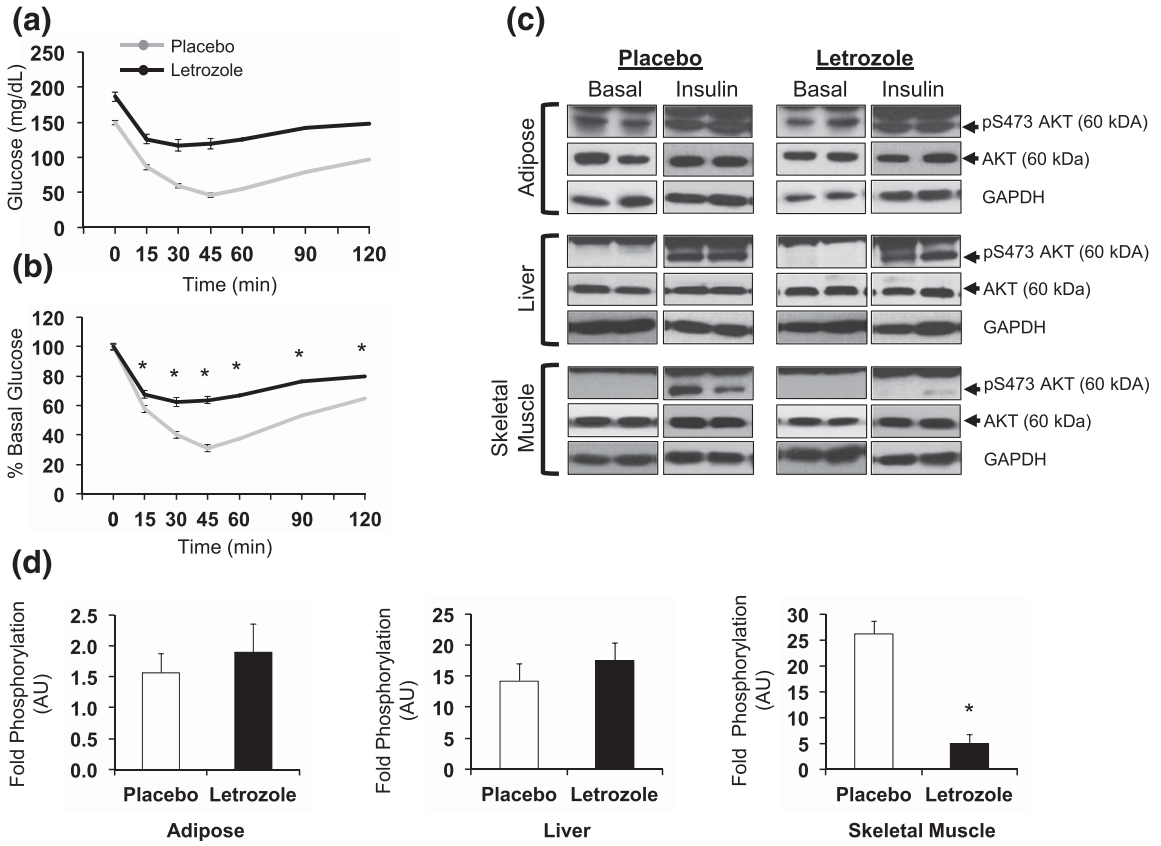

Figure 4. Insulin sensitivity was impaired after 5 weeks of letrozole treatment. (a) *In vivo* ITT was performed in fasted mice using an intraperitoneal injection of 0.75 U/kg insulin; (b) ITT data presented as percent of basal glucose. Error bars are included in (a) and (b), but some are too small to be seen; n = 10 to 11 per group, $*P < 0.05$ placebo vs letrozole by mixed-effects model. (c) Western blots of tissues from placebo- and letrozole-treated mice were used to assess AKT phosphorylation after an *ex vivo* insulin challenge. Each image presents two mice per group, and images are representative of three to four mice per group. (d) Quantification of data in (c) by densitometry; $*P < 0.05$ by *t* test. GAPDH, glyceraldehyde 3-phosphate dehydrogenase.

effect of letrozole after 5 weeks of treatment (43, 44), we found that testosterone was increased by approximately fivefold in letrozole-treated mice compared with placebo, whereas LH was 10-fold higher than placebo [Fig. 7(a) and 7(b)]. There was no statistical difference in 17β-estradiol levels between the two groups [Fig. 7(c)]. These data indicate that 1 week of letrozole treatment was sufficient to increase endogenous testosterone levels.

Table 1. Letrozole-Treated Mice With Dyslipidemia

Blood Test (Units)	Placebo	Letrozole
Cholesterol (mg/dL)	114 ± 2	140 ± 4[a]
HDL (mg/mL)	85 ± 2	103 ± 1[a]
Triglycerides (mg/dL)	85 ± 4	127 ± 6[a]
Free fatty acids (mEq/L)	0.72 ± 0.02	0.79 ± 0.03[b]
Leptin (ng/mL)	3.1 ± 0.9	17.1 ± 1.7[a]
IL-6 (pg/mL)	70.4 ± 23.8	78.4 ± 23.6

Mice were treated with placebo or letrozole for 5 weeks and then were fasted for 6 hours prior to blood collection; n = 9 to 12 per group. Values are presented as mean ± standard error of the mean.

[a] $P < 0.0001$ by *t* test.

[b] $P < 0.05$ by *t* test.

Glucose homeostasis was mildly disrupted after 1 week of letrozole treatment

Because the mice were mildly hyperglycemic and hyperinsulinemic after 1 week of letrozole treatment, we assessed whether there were defects in *in vivo* GSIS. Although more modest than what was observed at 5 weeks, 1 week of letrozole treatment resulted in an increase in FBG [Fig. 8(a) and 8(b)] and delayed disposal of exogenous glucose over 2 hours [Fig. 8(c)]. The amount of insulin secretion in response to exogenous glucose was similar between placebo- and letrozole-treated mice [Fig. 8(d) and 8(e)]. These data suggest that the defect in GSIS observed after 5 weeks of letrozole treatment developed after 1 week of treatment.

Interestingly, unlike mice treated for 5 weeks with letrozole, serum glucagon was elevated in fasted mice treated with letrozole for 1 week despite the presence of hyperglycemia and hyperinsulinemia [Fig. 8(f)]. These data suggest that inappropriate secretion of glucagon or, alternatively, impaired clearance could contribute to the initial hyperglycemia that occurs after 1 week of letrozole treatment in this model.

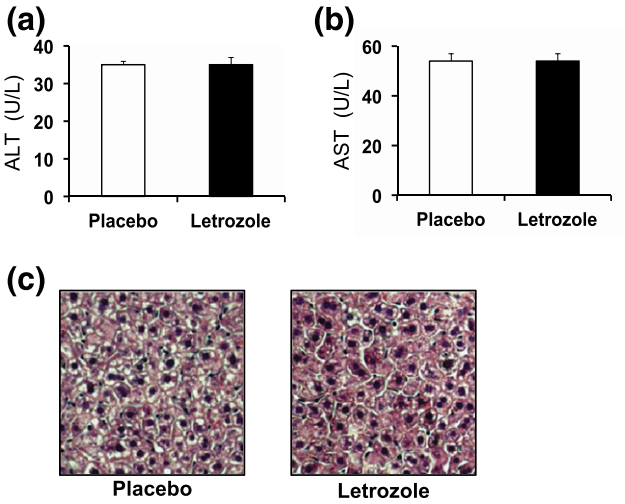

Figure 5. Liver enzymes and histology were normal after 5 weeks of letrozole treatment. (a) Fasting serum ALT and (b) AST; n = 7 to 9 per group. (c) Representative image of hematoxylin and eosin–stained liver sections from placebo- or letrozole-treated mice after 5 weeks of treatment; ×20 objective; n = 3 per group.

Insulin resistance was present but no different from placebo after 1 week of letrozole treatment

Because mice had fasting hyperinsulinemia and hyperglycemia after 1 week of letrozole treatment, we assessed insulin sensitivity at this time point by ITT. Letrozole-treated mice displayed a similar reduction in blood glucose in response to exogenous insulin as placebo-treated mice [Fig. 9(a) and 9(b)]. At 5 weeks of age (1 week of treatment), both groups had a modest reduction in blood glucose to 75% of FBG levels [Fig. 9(b)], demonstrating puberty-induced insulin resistance. This is in contrast to 9 weeks of age (5 weeks of treatment), where blood glucose in placebo-treated mice dropped to 35% of FBG values. Thus, although insulin resistance was present in both placebo- and letrozole-treated mice at 1 week of treatment, they displayed the same sensitivity to exogenous insulin, indicating that 1 week of letrozole treatment did not result in pathologic insulin resistance.

Proposed model of the progression of metabolic changes in the letrozole-induced PCOS mouse model

Our study demonstrated that raising endogenous testosterone levels using the aromatase inhibitor, letrozole, resulted in multiple metabolic features similar to those found in many women with PCOS, including mild hyperglycemia, hyperinsulinemia, insulin resistance, and dyslipidemia. The model presented in Fig. 10 contrasts the normal metabolic changes that occur during puberty in placebo-treated mice vs the metabolic dysregulation observed in letrozole-treated mice. Puberty is a period of transient insulin resistance that arises as a physiologic adaptation to puberty that resolves by adulthood. Insulin sensitivity decreases by approximately 30% during puberty, and insulin secretion

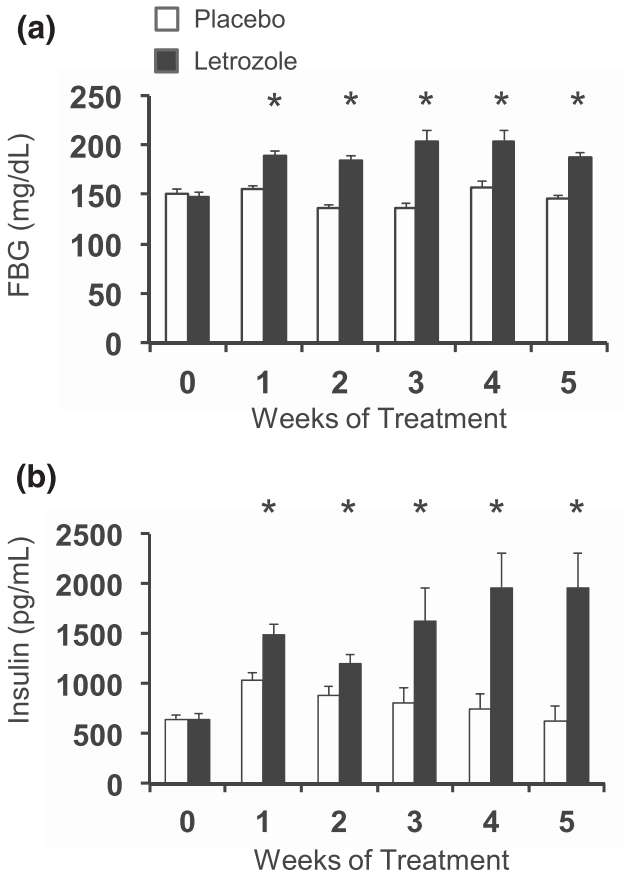

Figure 6. Hyperglycemia and hyperinsulinemia were present after 1 week of letrozole treatment. FBG and insulin were measured weekly in mice. (a) FBG was elevated after 1 week of letrozole treatment; n = 16 to 19 per group for weeks 0 to 2 and 5, n = 6 to 7 per group for weeks 3 and 4. (b) Hyperinsulinemia was present after 1 week of treatment. n = 16 to 19 per group for weeks 0 to 2, n = 6 to 7 per group for weeks 3 to 5; $*P < 0.05$ placebo vs letrozole by mixed-effects model analysis. Analysis of placebo insulin values demonstrated that weeks 1 and 2 were significantly different from week 0 using a one-way analysis of variance with *post hoc* Tukey test, $P < 0.05$.

increases to maintain a euglycemic state, and this is consistent with our data (54, 56). We observed an increase in insulin secretion near the beginning of puberty in placebo-treated mice, between 4 and 5 weeks of age (Fig. 6). We also observed insulin resistance at 4 weeks of age in placebo-treated mice (Fig. 9) that resolved by 9 weeks of age (Fig. 4). In contrast, letrozole treatment of pubertal mice resulted in hyperandrogenemia and a decompensated metabolic state that included hyperglycemia, hyperinsulinemia, and insulin resistance at 9 weeks of age.

Discussion

PCOS is a heterogeneous, polygenic disorder that often results in metabolic perturbation as well as impairment of the reproductive axis (57). Recently, we reported that letrozole treatment of pubertal female mice resulted in hallmarks of PCOS, including hyperandrogenism,

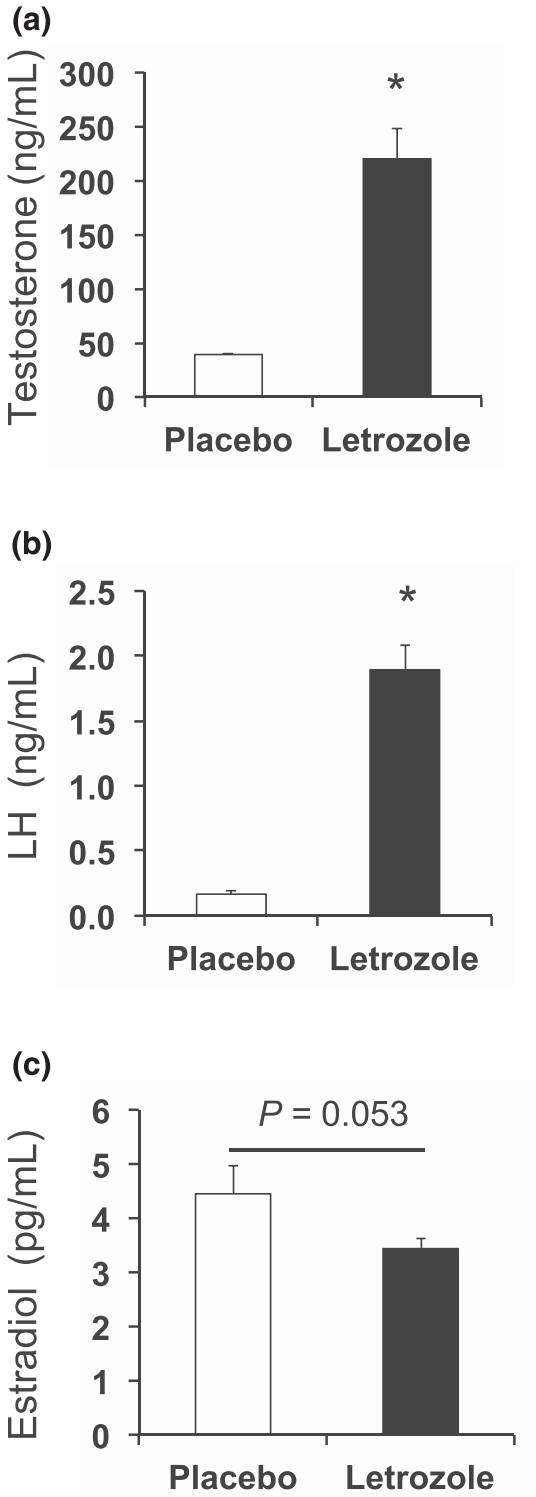

Figure 7. Reproductive hormones changed after 1 week of letrozole treatment. Both (a) testosterone and (b) LH were increased by 1 week of letrozole treatment (5 weeks of age) in nonfasted mice. (c) 17β-Estradiol was not statistically different; n = 8 per group; *$P < 0.05$ by *t* test.

anovulation, and polycystic ovaries (43). This letrozole-induced PCOS mouse model also exhibited weight gain due to increased abdominal adiposity as well as elevated FBG levels and mild glucose intolerance (44). Notably, the persistent hyperandrogenemia and anovulation in this model are similar to the phenotype of PCOS women diagnosed with hyperandrogenism and ovulatory dysfunction. This is in contrast to models that impose a hyperandrogenic insult during prenatal or postnatal development that does not result in elevated androgens during the time of metabolic assessment. Because hyperandrogenism is significantly associated with development of a metabolic phenotype in women with PCOS (2, 23, 24), we further investigated the metabolic dysfunction that occurs in this model of androgen excess. We report that letrozole treatment resulted in multiple, additional metabolic abnormalities associated with PCOS, including basal hyperinsulinemia, blunted GSIS, insulin resistance, and dyslipidemia. Notably, this metabolic dysregulation occurred without a change in diet, food intake, or total energy expenditure (Fig. 1). In addition, we demonstrated that hyperinsulinemia and mild hyperglycemia occurred after 1 week of letrozole treatment, prior to weight gain and the development of insulin resistance, indicating that this model may be useful for understanding how metabolic dysregulation develops in women after establishment of a hyperandrogenic milieu.

One of the striking findings in our study was that letrozole treatment of pubertal female mice resulted in elevated fasting insulin levels without evidence of pathologic insulin resistance after 1 week of treatment (Fig. 6). Metabolic parameters in rodent hyperandrogenic PCOS models were typically evaluated at the conclusion of the study and rarely measured in the early stages of exposure as we did in our study. For instance, when female mice were treated with testosterone from postnatal days (PNDs) 10 to 24, an increase in fat mass was noted in the testosterone-treated mice at 6 weeks of age, but no earlier metabolic hormone assessments were performed (58). Similarly, in female mice that received DHEA treatment at PNDs 23 to 43, metabolic assessment of the DHEA-treated mice demonstrated increased weight, hyperinsulinemia, and hyperglycemia at PND 43 (41). The data from these models are consistent with our findings that hyperandrogenemia correlates with increased fasting insulin and glucose levels, but it is unclear in these models if hyperinsulinemia and hyperglycemia develop prior to weight gain and insulin resistance. Although basal hyperinsulinemia in women with PCOS has been primarily attributed to compensatory insulin secretion in response to insulin resistance (59), our data do not support this hypothesis but rather support the idea that hyperinsulinemia may develop prior to insulin resistance. This idea is also supported by a recent study by Andrisse *et al.* (60) that reported increased fasting insulin levels after 1 week of DHT treatment in adult female mice without any weight gain.

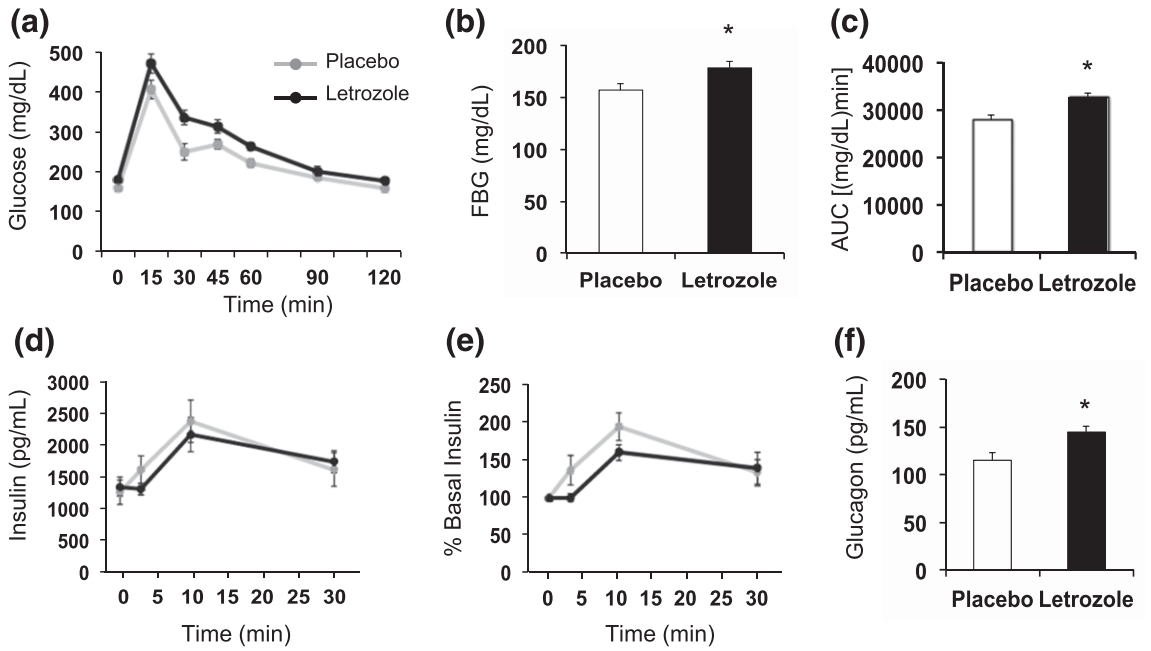

Figure 8. Glucose homeostasis was mildly altered after 1 week of letrozole treatment. (a–e) *In vivo* GSIS test; n = 8 per group. (a) Changes in blood glucose over time during GSIS. (b) FBG was increased in letrozole-treated mice; $*P < 0.05$ by *t* test. (c) Blood glucose area under the curve (AUC) was increased in letrozole-treated mice; $*P < 0.05$ by *t* test. (d) Serum insulin levels during GSIS and (e) percent relative to basal insulin demonstrated that insulin secretion in response to exogenous glucose stimulation was not statistically different between groups. Serum insulin levels were significantly increased at 10 minutes postinjection; $*P < 0.05$ by one-way repeated-measures analysis of variance. (f) Fasting glucagon was increased in letrozole-treated mice; $*P < 0.05$ by *t* test.

Women with PCOS are reported to have basal hyperinsulinemia, along with blunted insulin secretion in response to food or glucose, which is suggestive of pancreatic β-cell dysfunction (3, 9, 61–64). In addition to basal hyperinsulinemia, we also observed a significantly decreased insulin response to a bolus of glucose in letrozole-treated mice compared with placebo-treated mice after 5 weeks of letrozole [Fig. 2(e)]. These data are similar to what was observed in female rats treated at PND 21 with DHT for 90 days. In this study, an *in vivo* GSIS test showed that DHT treatment resulted in a significantly blunted insulin secretion in response to glucose (65). Notably, although we observed basal fasting hyperinsulinemia and a blunted *in vivo* GSIS in the letrozole-treated mice, other hyperinsulinemic mouse models using male mice were reported to exhibit a normal GSIS in the context of significant hyperinsulinemia (51, 66). Thus, the fourfold higher fasting insulin levels that occurred in the letrozole-induced PCOS model would not necessarily preclude a glucose-stimulated release of insulin, suggesting that the blunted GSIS observed after 5 weeks of letrozole treatment is due to β-cell dysfunction.

In contrast to the *in vivo* GSIS, we observed a similar amount of insulin secretion when cultured pancreatic islets isolated from placebo- and letrozole-treated mice were stimulated with high levels of glucose in the absence or presence of DHT [Fig. 3(b)]. Similar to a previous report (65), islets from male mice cultured with DHT had an increased GSIS response, whereas islets from female mice did not [Fig. 3(a)], indicating that islets from letrozole-treated mice responded to DHT as if they were female islets. Although multiple clinical studies have demonstrated a significant association between elevated androgens and β-cell dysfunction in women with PCOS, only a few studies have investigated the effect of excess androgens on female pancreatic β-cells (38, 65, 67). The androgen receptor (AR) is expressed in normal female human and mouse pancreas (51, 68, 69). In contrast to our results, DHT treatment of pancreatic islets isolated from female mice treated prenatally with androgens resulted in a small reduction in insulin secretion in response to high glucose (38). Cultured pancreatic islets isolated from female rats and treated with either testosterone or DHT were also reported to have lower GSIS rates than vehicle controls (65). Our data suggest that androgens do not have a direct effect on insulin secretion in β-cells in the letrozole-induced PCOS mouse model, although it is still possible that activation of AR in β-cells results in insulin hypersecretion via alternative mechanisms. Future studies employing a β-cell knockout of AR will be required to determine whether AR in β-cells is required for the hyperinsulinemia and blunted GSIS observed in letrozole-treated female mice. In addition, it will be interesting to determine whether letrozole treatment causes β-cell proliferation and expansion and if this is AR dependent. Furthermore, although our model

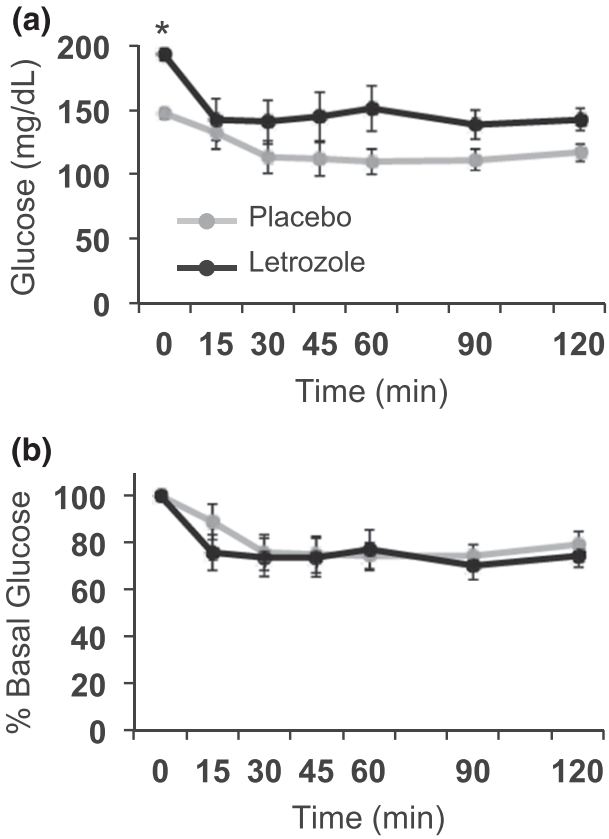

Figure 9. Insulin resistance was similar in placebo- and letrozole-treated mice after 1 week of treatment. (a, b) An ITT was conducted on mice after 1 week of treatment. (a) Changes in glucose levels in response to exogenous insulin during ITT. (b) ITT data presented as percent of basal glucose.

mimics the hyperinsulinemia and β-cell dysfunction observed in women with PCOS, decreased hepatic insulin clearance is reported to contribute to the hyperinsulinemia in women with PCOS, particularly in obese women (17, 70–72). Additional studies will be required to determine whether hepatic clearance of insulin is decreased in the letrozole-induced PCOS mouse model.

Because insulin resistance is a key feature of metabolic dysfunction in PCOS, we evaluated whether letrozole treatment of pubertal female mice resulted in insulin resistance. Despite elevated fasting basal insulin and glucose levels, placebo- and letrozole-treated mice were equally insulin sensitive after 1 week of treatment, whereas significant insulin resistance was present in letrozole-treated mice after 5 weeks of treatment (Figs. 4 and 9). Although insulin resistance in PCOS is independent of body mass index, it has been reported that obese women with PCOS have greater insulin resistance than lean women due to the additive effect of obesity on insulin resistance (16, 17, 72–74). Future studies will be required to determine when insulin resistance develops in this model. In addition to a decreased responsiveness to insulin, molecular markers of insulin resistance have been identified in the skeletal muscle of women with PCOS (75, 76). Skeletal muscle biopsies from women with PCOS in a euglycemic-hyperinsulinemic clamp study were reported to have attenuated phosphorylation of AKT S473 and T308 in response to insulin (76). Interestingly, after 5 weeks of letrozole treatment, we observed a decrease in insulin-induced phosphorylation of AKT S473 in skeletal muscle but not in liver or parametrial adipose tissue (Fig. 4), indicating that insulin resistance in skeletal muscle may occur in the letrozole-induced PCOS mouse model. Future studies using a euglycemic-hyperinsulinemic clamp will be necessary to establish the temporal and tissue pattern of insulin resistance in the letrozole-induced PCOS mouse model, as well as the degree of insulin resistance.

In addition to β-cell dysfunction and insulin resistance, one-third of women with PCOS in the United States have dysglycemia, which is defined as prediabetes and diabetes (77, 78). Prediabetes is a condition in which blood glucose is elevated but does not meet the diagnostic threshold of diabetes. Dysglycemia can be detected by an abnormal oral GTT, elevated hemoglobin A1C, and/or increased FBG. As previously reported (27, 43, 44), the letrozole-induced PCOS mouse model exhibits dysglycemia, with elevated FBG and impaired glucose tolerance [Fig. 2 and Fig. 6(a)]. Because FBG levels in mice are strain dependent (27), there is no consensus on glycemic values to distinguish prediabetic- or diabetic-like states in mice. Letrozole treatment of pubertal female mice resulted in mild hyperglycemia, with FBG levels 18% to 30% greater than controls over the 5 weeks of treatment. With mild fasting hyperglycemia and abnormal glucose tolerance, without clear signs of diabetes, our model is consistent with the dysglycemia found in women with PCOS and reflects a prediabetic-like phenotype.

Increased adiposity is a common finding in women with PCOS, with 80% in the United States being overweight or obese (4). Not surprisingly, 70% of women with PCOS demonstrate some level of dyslipidemia

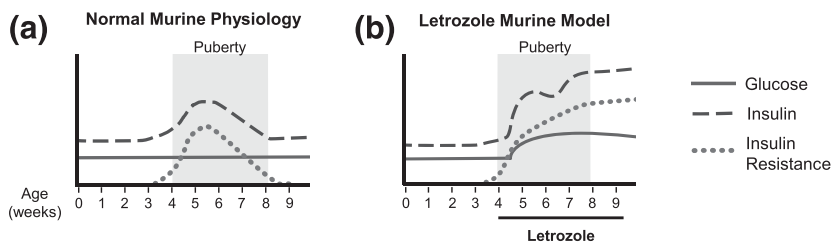

Figure 10. Model of metabolic dysregulation in the letrozole-induced PCOS mouse model. (a) Puberty results in an insulin-resistant state, with euglycemia, that resolves by adulthood. (b) Letrozole treatment during puberty increases endogenous testosterone and results in metabolic dysfunction.

consisting of elevated triglycerides, free fatty acids, total cholesterol, and low-density lipoprotein, along with low HDL. Dyslipidemia in PCOS women is also strongly associated with hyperandrogenism and insulin resistance (12, 14, 15, 53, 79, 80). In addition, obesity, insulin resistance, and dyslipidemia place women with PCOS at risk for NAFLD (20). In addition to increased weight and insulin resistance, the letrozole-induced PCOS mouse model exhibited dyslipidemia after 5 weeks of treatment (Table 1) but had no signs of NAFLD (Fig. 5). Letrozole-treated mice weighed 14% to 19% more than placebo-treated mice after 2 to 5 weeks of treatment [Fig. 1(b)], primarily due to increased visceral adiposity, and had a 5.5-fold increase in fasting leptin levels (Table 1). Our previous study also demonstrated adipocyte hypertrophy, macrophage infiltration, and an increase in inflammatory markers in parametrial adipose tissue (43). The dyslipidemia observed in the letrozole-treated mice was consistent with changes in women with PCOS, with the exception of elevated HDL levels. It is possible that the elevated HDL measured after 5 weeks of letrozole treatment reflects a transient compensatory rise due to elevated triglycerides (81, 82) or to increased steroidogenesis because rodents preferentially use HDL for this process (83). It is notable that the dyslipidemia observed after 5 weeks of letrozole treatment did not affect the liver as evident by normal AST and ALT, along with normal histology. Future studies are necessary to determine if prolonging the model will result in ectopic lipid accumulation in the liver and a NAFLD-like state. Thus, our data demonstrating increased adiposity and dyslipidemia in the letrozole-induced PCOS mouse model suggest that this model represents an overweight/obese PCOS phenotype and that it will be useful in understanding how hyperandrogenism results in changes in adiposity and lipid profiles.

Progression of the pathology in the letrozole-induced PCOS mouse model was rapid, with hyperinsulinemia and mild hyperglycemia occurring with documented hyperandrogenemia after 1 week of letrozole treatment and prior to pathologic insulin resistance. This model implies that insulin resistance in PCOS may not be causal for hyperinsulinemia. In addition, this model suggests that insulin resistance in PCOS might arise from sustained hyperinsulinemia and hyperglycemia resulting in increased adiposity and low-grade, chronic tissue inflammation (43, 84). Because significant reproductive and metabolic hormone changes occur during puberty (22, 85–89), it is likely that letrozole treatment during this developmental period increased the severity of the metabolic phenotype. Notably, the metabolic dysregulation induced by hyperandrogenemia occurred in the context of pubertal insulin resistance, which has been reported to increase the risk of developing type 2 diabetes and cardiovascular disease in adolescents along with accelerating the complications of diabetes (85, 90–92). Future studies applying this experimental model to adult female mice with normal insulin sensitivity will be useful for investigating the role of puberty in the development of the PCOS metabolic phenotype. Genetic background is also a probable contributor to the severity of the phenotype as C57BL/6 mice are obesity prone (93, 94) and display varying glucose responses even within substrains (27).

Because PCOS is a heterogeneous disorder, it has been challenging to develop animal models that fully recapitulate both the reproductive and metabolic phenotypes. Our study demonstrates that the letrozole-induced PCOS mouse model has many features of the PCOS metabolic phenotype, including obesity, hyperinsulinemia, insulin resistance, mild hyperglycemia, and dyslipidemia, and therefore may be a good model for women with PCOS who have biochemical/clinical hyperandrogenism and are overweight/obese. Although it is now becoming evident that steroid hormone action in metabolism is sex specific, there is a fundamental lack of understanding of how hyperandrogenemia affects female metabolism (67, 95). The development of hyperandrogenic female mouse models will facilitate studies investigating mechanisms of androgen action in female metabolic tissues. In particular, the combination of tissue-specific AR knockout mice with the letrozole-induced PCOS mouse model will allow researchers to define the contribution of excess AR activation to PCOS metabolic dysfunction within a specific organ or cell type.

Acknowledgments

We thank Shannon Stephens, Erica Schoeller, Bryan Ho, and Pedro Torres for their technical expertise and assistance. We thank Kellie Breen-Church, Scott Kelley, and Pedro Torres for their comments and suggestions on the manuscript. Hormone levels were measured by the University of Virginia, Center for Research in Reproduction, Ligand Assay and Analysis Core Facility (P50 HD28934).

Address all correspondence and requests for reprints to: Varykina G. Thackray, PhD, Department of Reproductive Medicine, University of California, San Diego, 9500 Gilman Drive, La Jolla, California 92093-0674. E-mail: vthackray@ucsd.edu.

This work was funded by the National Institute of Child Health and Human Development through Grant R01 HD067448 (to V.G.T.), a cooperative agreement as part of the National Centers for Translational Research in Reproduction and Infertility (P50HD012303), and Grants T32 HD007203 and F32 HD074414 (to D.V.S.). D.V.S. and A.H-C. were funded by National Institute of General Medical Sciences Grant K12 GM068524.

Appendix. Antibody Table

Protein Target	Name of Antibody	Manufacturer, Catalog No.	Species Raised in; Monoclonal or Polyclonal	Dilution Used	RRID
AKT	AKT1/2/3 (H-136)	Santa Cruz Biotechnology, sc8312	Rabbit; polyclonal	1:3000	AB_671714
AKT	Phospho-Akt (Ser473) (587F11)	Cell Signaling Technology, 4051	Mouse; monoclonal	1:2000	AB_331158
GAPDH	GAPDH (FL-335)	Santa Cruz Biotechnology, sc25778	Rabbit; polyclonal	1:3000	AB_10167668

Abbreviation: GAPDH, glyceraldehyde 3-phosphate dehydrogenase.

Disclosure Summary: The authors have nothing to disclose.

References

1. Fauser BC, Tarlatzis BC, Rebar RW, Legro RS, Balen AH, Lobo R, Carmina E, Chang J, Yildiz BO, Laven JS, Boivin J, Petraglia F, Wijeyeratne CN, Norman RJ, Dunaif A, Franks S, Wild RA, Dumesic D, Barnhart K. 2012 Consensus on women's health aspects of polycystic ovary syndrome (PCOS): the Amsterdam ESHRE/ASRM-Sponsored 3rd PCOS Consensus Workshop Group. *Fertil Steril*. **97**:28–38.e25.
2. Lizneva D, Suturina L, Walker W, Brakta S, Gavrilova-Jordan L, Azziz R. Criteria, prevalence, and phenotypes of polycystic ovary syndrome. *Fertil Steril*. 2016;**106**(1):6–15.
3. Azziz R, Carmina E, Chen Z, Dunaif A, Laven JSE, Legro RS, Lizneva D, Natterson-Horowtiz B, Teede HJ, Yildiz BO. Polycystic ovary syndrome. *Nat Rev Dis Primers*. 2016;**2**:16057.
4. Dumesic DA, Oberfield SE, Stener-Victorin E, Marshall JC, Laven JS, Legro RS. Scientific statement on the diagnostic criteria, epidemiology, pathophysiology, and molecular genetics of polycystic ovary syndrome. *Endocr Rev*. 2015;**36**(5):487–525.
5. Azziz R, Adashi EY. Stein and Leventhal: 80 years on. *Am J Obstet Gynecol*. 2016;**214**(2):247.e1–247.e11.
6. Stein IF, Leventhal ML. Amenorrhea associated with bilateral polycystic ovaries. *Am J Obstet Gynecol*. 1935;**29**:181–191.
7. Diamanti-Kandarakis E, Dunaif A. Insulin resistance and the polycystic ovary syndrome revisited: an update on mechanisms and implications. *Endocr Rev*. 2012;**33**(6):981–1030.
8. Dunaif A, Fauser BC. Renaming PCOS—a two-state solution. *J Clin Endocrinol Metab*. 2013;**98**(11):4325–4328.
9. Dunaif A, Finegood DT. Beta-cell dysfunction independent of obesity and glucose intolerance in the polycystic ovary syndrome. *J Clin Endocrinol Metab*. 1996;**81**(3):942–947.
10. Dunaif A, Segal KR, Shelley DR, Green G, Dobrjansky A, Licholai T. Evidence for distinctive and intrinsic defects in insulin action in polycystic ovary syndrome. *Diabetes*. 1992;**41**(10):1257–1266.
11. Ehrmann DA, Liljenquist DR, Kasza K, Azziz R, Legro RS, Ghazzi MN; PCOS/Troglitazone Study Group. Prevalence and predictors of the metabolic syndrome in women with polycystic ovary syndrome. *J Clin Endocrinol Metab*. 2006;**91**(1):48–53.
12. Yang R, Yang S, Li R, Liu P, Qiao J, Zhang Y. Effects of hyperandrogenism on metabolic abnormalities in patients with polycystic ovary syndrome: a meta-analysis. *Reprod Biol Endocrinol*. 2016;**14**(1):67.
13. Stepto NK, Cassar S, Joham AE, Hutchison SK, Harrison CL, Goldstein RF, Teede HJ. Women with polycystic ovary syndrome have intrinsic insulin resistance on euglycaemic-hyperinsulaemic clamp. *Hum Reprod*. 2013;**28**(3):777–784.
14. Diamanti-Kandarakis E, Papavassiliou AG, Kandarakis SA, Chrousos GP. Pathophysiology and types of dyslipidemia in PCOS. *Trends Endocrinol Metab*. 2007;**18**(7):280–285.
15. Göbl CS, Ott J, Bozkurt L, Feichtinger M, Rehmann V, Cserjan A, Heinisch M, Steinbrecher H, JustKukurova I, Tuskova R, Leutner M, Vytiska-Binstorfer E, Kurz C, Weghofer A, Tura A, Egarter C, Kautzky-Willer A. To assess the association between glucose metabolism and ectopic lipid content in different clinical classifications of PCOS. *PLoS One*. 2016;**11**(8):e0160571.
16. Pasquali R, Gambineri A. Glucose intolerance states in women with the polycystic ovary syndrome. *J Endocrinol Invest*. 2014;**36**(8):648–653.
17. Vrbíková J, Cibula D, Dvoráková K, Stanická S, Sindelka G, Hill M, Fanta M, Vondra K, Skrha J. Insulin sensitivity in women with polycystic ovary syndrome. *J Clin Endocrinol Metab*. 2004;**89**(6):2942–2945.
18. Churchill SJ, Wang ET, Pisarska MD. Metabolic consequences of polycystic ovary syndrome. *Minerva Ginecol*. 2015;**67**(6):545–555.
19. Goodman NF, Cobin RH, Futterweit W, Glueck JS, Legro RS, Carmina E; American Association of Clinical Endocrinologists (AACE); American College of Endocrinology (ACE); Androgen Excess and PCOS Society. American Association of Clinical Endocrinologists, American College of Endocrinology, and Androgen Excess and PCOS Society Disease State clinical review: guide to the best practices in the evaluation and treatment of polycystic ovary syndrome—part 2. *Endocr Pract*. 2015;**21**(12):1415–1426.
20. Vassilatou E. Nonalcoholic fatty liver disease and polycystic ovary syndrome. *World J Gastroenterol*. 2014;**20**(26):8351–8363.
21. Hart R, Doherty DA. The potential implications of a PCOS diagnosis on a woman's long-term health using data linkage. *J Clin Endocrinol Metab*. 2015;**100**(3):911–919.
22. Moran LJ, Misso ML, Wild RA, Norman RJ. Impaired glucose tolerance, type 2 diabetes and metabolic syndrome in polycystic ovary syndrome: a systematic review and meta-analysis. *Hum Reprod Update*. 2010;**16**(4):347–363.
23. Barber TM, Wass JA, McCarthy MI, Franks S. Metabolic characteristics of women with polycystic ovaries and oligo-amenorrhoea but normal androgen levels: implications for the management of polycystic ovary syndrome. *Clin Endocrinol (Oxf)*. 2007;**66**(4):513–517.
24. Moghetti P, Tosi F, Bonin C, Di Sarra D, Fiers T, Kaufman J-M, Giagulli VA, Signori C, Zambotti F, Dall'Alda M, Spiazzi G, Zanolin ME, Bonora E. Divergences in insulin resistance between the different phenotypes of the polycystic ovary syndrome. *J Clin Endocrinol Metab*. 2013;**98**(4):E628–E637.
25. Abbott DH, Bacha F. Ontogeny of polycystic ovary syndrome and insulin resistance in utero and early childhood. *Fertil Steril*. 2013;**100**(1):2–11.
26. Barber TM, Franks S. Genetics of polycystic ovary syndrome. *Front Horm Res*. 2012;**40**:28–39.
27. Berglund ED, Li CY, Poffenberger G, Ayala JE, Fueger PT, Willis SE, Jewell MM, Powers AC, Wasserman DH. Glucose metabolism in vivo in four commonly used inbred mouse strains. *Diabetes*. 2008;**57**(7):1790–1799.
28. Franks S, Berga SL. Does PCOS have developmental origins? *Fertil Steril*. 2012;**97**(1):2–6.
29. Legro RS, Driscoll D, Strauss JF III, Fox J, Dunaif A. Evidence for a genetic basis for hyperandrogenemia in polycystic ovary syndrome. *Proc Natl Acad Sci USA*. 1998;**95**(25):14956–14960.
30. Vink JM, Sadrzadeh S, Lambalk CB, Boomsma DI. Heritability of polycystic ovary syndrome in a Dutch twin-family study. *J Clin Endocrinol Metab*. 2006;**91**(6):2100–2104.

31. Padmanabhan V, Veiga-Lopez A. Animal models of the polycystic ovary syndrome phenotype. *Steroids*. 2013;**78**(8):734–740.
32. Shi D, Vine DF. Animal models of polycystic ovary syndrome: a focused review of rodent models in relationship to clinical phenotypes and cardiometabolic risk. *Fertil Steril*. 2012;**98**(1):185–193.e2.
33. van Houten EL, Visser JA. Mouse models to study polycystic ovary syndrome: a possible link between metabolism and ovarian function? *Reprod Biol*. 2014;**14**(1):32–43.
34. Walters KA, Allan CM, Handelsman DJ. Rodent models for human polycystic ovary syndrome. *Biol Reprod*. 2012;**86**(5):149, 1–12.
35. Walters KA. Androgens in polycystic ovary syndrome: lessons from experimental models. *Curr Opin Endocrinol Diabetes Obes*. 2016; **23**(3):257–263.
36. Caldwell ASL, Middleton LJ, Jimenez M, Desai R, McMahon AC, Allan CM, Handelsman DJ, Walters KA. Characterization of reproductive, metabolic, and endocrine features of polycystic ovary syndrome in female hyperandrogenic mouse models. *Endocrinology*. 2014;**155**(8):3146–3159.
37. Moore AM, Prescott M, Campbell RE. Estradiol negative and positive feedback in a prenatal androgen-induced mouse model of polycystic ovarian syndrome. *Endocrinology*. 2013;**154**(2): 796–806.
38. Roland AV, Nunemaker CS, Keller SR, Moenter SM. Prenatal androgen exposure programs metabolic dysfunction in female mice. *J Endocrinol*. 2010;**207**(2):213–223.
39. Witham EA, Meadows JD, Shojaei S, Kauffman AS, Mellon PL. Prenatal exposure to low levels of androgen accelerates female puberty onset and reproductive senescence in mice. *Endocrinology*. 2012;**153**(9):4522–4532.
40. van Houten EL, Kramer P, McLuskey A, Karels B, Themmen AP, Visser JA. Reproductive and metabolic phenotype of a mouse model of PCOS. *Endocrinology*. 2012;**153**(6):2861–2869.
41. Solano ME, Sander VA, Ho H, Motta AB, Arck PC. Systemic inflammation, cellular influx and up-regulation of ovarian VCAM-1 expression in a mouse model of polycystic ovary syndrome (PCOS). *J Reprod Immunol*. 2011;**92**(1–2):33–44.
42. Sander V, Luchetti CG, Solano ME, Elia E, Di Girolamo G, Gonzalez C, Motta AB. Role of the N, N′-dimethylbiguanide metformin in the treatment of female prepuberal BALB/c mice hyperandrogenized with dehydroepiandrosterone. *Reproduction*. 2006;**131**(3):591–602.
43. Kauffman AS, Thackray VG, Ryan GE, Tolson KP, Glidewell-Kenney CA, Semaan SJ, Poling MC, Iwata N, Breen KM, Duleba AJ, Stener-Victorin E, Shimasaki S, Webster NJ, Mellon PL. A novel letrozole model recapitulates both the reproductive and metabolic phenotypes of polycystic ovary syndrome in female mice. *Biol Reprod*. 2015;**93**(3):69.
44. Kelley ST, Skarra DV, Rivera AJ, Thackray VG. The gut microbiome is altered in a letrozole-induced mouse model of polycystic ovary syndrome. *PLoS One*. 2016;**11**(1):e0146509.
45. Fueger PT, Hernandez AM, Chen Y-C, Colvin ES. Assessing replication and beta cell function in adenovirally-transduced isolated rodent islets. *J Vis Exp*. 2012;(64):4080.
46. Ayala JE, Samuel VT, Morton GJ, Obici S, Croniger CM, Shulman GI, Wasserman DH, McGuinness OP; NIH Mouse Metabolic Phenotyping Center Consortium. Standard operating procedures for describing and performing metabolic tests of glucose homeostasis in mice. *Dis Model Mech*. 2010;**3**(9–10):525–534.
47. Osborn O, Oh DY, McNelis J, Sanchez-Alavez M, Talukdar S, Lu M, Li P, Thiede L, Morinaga H, Kim JJ, Heinrichsdorff J, Nalbandian S, Ofrecio JM, Scadeng M, Schenk S, Hadcock J, Bartfai T, Olefsky JM. G protein-coupled receptor 21 deletion improves insulin sensitivity in diet-induced obese mice. *J Clin Invest*. 2012;**122**(7):2444–2453.
48. Locascio JJ, Atri A. An overview of longitudinal data analysis methods for neurological research. *Dement Geriatr Cogn Dis Extra*. 2011;**1**(1):330–357.
49. Saltiel AR, Kahn CR. Insulin signalling and the regulation of glucose and lipid metabolism. *Nature*. 2001;**414**(6865):799–806.
50. Unger RH, Orci L. Paracrinology of islets and the paracrinopathy of diabetes. *Proc Natl Acad Sci USA*. 2010;**107**(37):16009–16012.
51. Navarro G, Xu W, Jacobson DA, Wicksteed B, Allard C, Zhang G, De Gendt K, Kim SH, Wu H, Zhang H, Verhoeven G, Katzenellenbogen JA, Mauvais-Jarvis F. Extranuclear actions of the androgen receptor enhance glucose-stimulated insulin secretion in the male. *Cell Metab*. 2016;**23**(5):837–851.
52. Boucher J, Kleinridders A, Kahn CR. Insulin receptor signaling in normal and insulin-resistant states. *Cold Spring Harb Perspect Biol*. 2014;**6**(1):a009191.
53. Rocha MP, Marcondes JAM, Barcellos CRG, Hayashida SAY, Curi DDG, da Fonseca ÂM, Bagnoli VR, Baracat EC. Dyslipidemia in women with polycystic ovary syndrome: incidence, pattern and predictors. *Gynecol Endocrinol*. 2010;**27**(10):814–819.
54. Goran MI, Gower BA. Longitudinal study on pubertal insulin resistance. *Diabetes*. 2001;**50**(11):2444–2450.
55. Nelson JF, Karelus K, Felicio LS, Johnson TE. Genetic influences on the timing of puberty in mice. *Biol Reprod*. 1990;**42**(4):649–655.
56. Moran A, Jacobs DR Jr, Steinberger J, Hong CP, Prineas R, Luepker R, Sinaiko AR. Insulin resistance during puberty: results from clamp studies in 357 children. *Diabetes*. 1999;**48**(10): 2039–2044.
57. Goodarzi MO, Dumesic DA, Chazenbalk G, Azziz R. Polycystic ovary syndrome: etiology, pathogenesis and diagnosis. *Nat Rev Endocrinol*. 2011;**7**(4):219–231.
58. Nohara K, Waraich RS, Liu S, Ferron M, Waget A, Meyers MS, Karsenty G, Burcelin R, Mauvais-Jarvis F. Developmental androgen excess programs sympathetic tone and adipose tissue dysfunction and predisposes to a cardiometabolic syndrome in female mice. *Am J Physiol Endocrinol Metab*. 2013;**304**(12):E1321–E1330.
59. Rosenfield RL, Ehrmann DA. The pathogenesis of polycystic ovary syndrome (PCOS): The hypothesis of PCOS as functional ovarian hyperandrogenism revisited. *Endocr Rev*. 2016;**37**(5):467–520.
60. Andrisse S, Childress S, Ma Y, Billings K, Chen Y, Xue P, Stewart A, Sonko ML, Wolfe A, Wu S. Low-dose dihydrotestosterone drives metabolic dysfunction via cytosolic and nuclear hepatic androgen receptor mechanisms. *Endocrinology*. 2017;**158**(3):531–544.
61. Ehrmann DA, Sturis J, Byrne MM, Karrison T, Rosenfield RL, Polonsky KS. Insulin secretory defects in polycystic ovary syndrome: relationship to insulin sensitivity and family history of non-insulin-dependent diabetes mellitus. *J Clin Invest*. 1995;**96**(1): 520–527.
62. Malin SK, Kirwan JP, Sia CL, González F. Pancreatic β-cell dysfunction in polycystic ovary syndrome: role of hyperglycemia-induced nuclear factor–κB activation and systemic inflammation. *Am J Physiol Endocrinol Metab*. 2015;**308**(9):E770–E777.
63. O'Meara NM, Blackman JD, Ehrmann DA, Barnes RB, Jaspan JB, Rosenfield RL, Polonsky KS. Defects in beta-cell function in functional ovarian hyperandrogenism. *J Clin Endocrinol Metab*. 1993;**76**(5):1241–1247.
64. Tao T, Li S, Zhao A, Mao X, Liu W. Early impaired β-cell function in Chinese women with polycystic ovary syndrome. *Int J Clin Exp Pathol*. 2012;**5**(8):777–786.
65. Wang H, Wang X, Zhu Y, Chen F, Sun Y, Han X. Increased androgen levels in rats impair glucose-stimulated insulin secretion through disruption of pancreatic beta cell mitochondrial function. *J Steroid Biochem Mol Biol*. 2015;**154**:254–266.
66. Wu H, Mezghenna K, Marmol P, Guo T, Moliner A, Yang S-N, Berggren P-O, Ibáñez CF. Differential regulation of mouse pancreatic islet insulin secretion and Smad proteins by activin ligands. *Diabetologia*. 2013;**57**(1):148–156.
67. Mauvais-Jarvis F. Role of sex steroids in β cell function, growth, and survival. *Trends Endocrinol Metab*. 2016;**27**(12):844–855.
68. Corbishley TP, Iqbal MJ, Wilkinson ML, Williams R. Androgen receptor in human normal and malignant pancreatic tissue and cell lines. *Cancer*. 1986;**57**(10):1992–1995.
69. Ruizeveld de Winter JA, Trapman J, Vermey M, Mulder E, Zegers ND, van der Kwast TH. Androgen receptor expression in human

tissues: an immunohistochemical study. *J Histochem Cytochem*. 1991;**39**(7):927–936.
70. Amato MC, Vesco R, Vigneri E, Ciresi A, Giordano C. Hyperinsulinism and polycystic ovary syndrome (PCOS): role of insulin clearance. *J Endocrinol Invest*. 2015;**38**(12):1319–1326.
71. Ciampelli M, Fulghesu AM, Cucinelli F, Pavone V, Caruso A, Mancuso S, Lanzone A. Heterogeneity in beta cell activity, hepatic insulin clearance and peripheral insulin sensitivity in women with polycystic ovary syndrome. *Hum Reprod*. 1997;**12**(9):1897–1901.
72. Mumm H, Altinok ML, Henriksen JE, Ravn P, Glintborg D, Andersen M. Prevalence and possible mechanisms of reactive hypoglycemia in polycystic ovary syndrome. *Hum Reprod*. 2016; **31**(5):1105–1112.
73. Dunaif A, Segal KR, Futterweit W, Dobrjansky A. Profound peripheral insulin resistance, independent of obesity, in polycystic ovary syndrome. *Diabetes*. 1989;**38**(9):1165–1174.
74. Holte J, Bergh T, Berne C, Berglund L, Lithell H. Enhanced early insulin response to glucose in relation to insulin resistance in women with polycystic ovary syndrome and normal glucose tolerance. *J Clin Endocrinol Metab*. 1994;**78**(5):1052–1058.
75. Corbould A, Kim Y-B, Youngren JF, Pender C, Kahn BB, Lee A, Dunaif A. Insulin resistance in the skeletal muscle of women with PCOS involves intrinsic and acquired defects in insulin signaling. *Am J Physiol Endocrinol Metab*. 2004;**288**(5):E1047–E1054.
76. Højlund K, Glintborg D, Andersen NR, Birk JB, Treebak JT, Frøsig C, Beck-Nielsen H, Wojtaszewski JFP. Impaired insulin-stimulated phosphorylation of Akt and AS160 in skeletal muscle of women with polycystic ovary syndrome is reversed by pioglitazone treatment. *Diabetes*. 2007;**57**(2):357–366.
77. Karakas SE, Kim K, Duleba AJ. Determinants of impaired fasting glucose versus glucose intolerance in polycystic ovary syndrome. *Diabetes Care*. 2010;**33**(4):887–893.
78. Legro RS, Kunselman AR, Dodson WC, Dunaif A. Prevalence and predictors of risk for type 2 diabetes mellitus and impaired glucose tolerance in polycystic ovary syndrome: a prospective, controlled study in 254 affected women. *J Clin Endocrinol Metab*. 1999;**84**(1): 165–169.
79. Csenteri OK, Sándor J, Kalina E, Bhattoa HP, Gődény S. The role of hyperinsulinemia as a cardiometabolic risk factor independent of obesity in polycystic ovary syndrome. *Gynecol Endocrinol*. 2017; **33**(1):34–38.
80. Wu Y, Zhang J, Wen Y, Wang H, Zhang M, Cianflone K. Increased acylation-stimulating protein, C-reactive protein, and lipid levels in young women with polycystic ovary syndrome. *Fertil Steril*. 2009; **91**(1):213–219.
81. Lindström T, Kechagias S, Carlsson M, Nystrom FH; Fast Food Study Group. Transient increase in HDL-cholesterol during weight gain by hyperalimentation in healthy subjects. *Obesity (Silver Spring)*. 2010;**19**(4):812–817.
82. Williams LM, Campbell FM, Drew JE, Koch C, Hoggard N, Rees WD, Kamolrat T, Thi Ngo H, Steffensen I-L, Gray SR, Tups A. The development of diet-induced obesity and glucose intolerance in C57BL/6 mice on a high-fat diet consists of distinct phases. *PLoS One*. 2014;**9**(8):e106159.
83. Hu J, Zhang Z, Shen W-J, Azhar S. Cellular cholesterol delivery, intracellular processing and utilization for biosynthesis of steroid hormones. *Nutr Metab (Lond)*. 2010;**7**:47.
84. Johnson AM, Olefsky JM. The origins and drivers of insulin resistance. *Cell*. 2013;**152**(4):673–684.
85. Kelsey MM, Zeitler PS. Insulin resistance of puberty. *Curr Diab Rep*. 2016;**16**(7):64.
86. Mouritsen A, Søeborg T, Hagen CP, Mieritz MG, Johannsen TH, Frederiksen H, Andersson A-M, Juul A. Longitudinal changes in serum concentrations of adrenal androgen metabolites and their ratios by LC-MS/MS in healthy boys and girls. *Clin Chim Acta*. 2015;**450**:370–375.
87. Reinehr T. Metabolic syndrome in children and adolescents: a critical approach considering the interaction between pubertal stage and insulin resistance. *Curr Diab Rep*. 2016;**16**(1):8.
88. Vryonidou A, Paschou SA, Muscogiuri G, Orio F, Goulis DG. Mechanisms in endocrinology: metabolic syndrome through the female life cycle. *Eur J Endocrinol*. 2015;**173**(5):R153–R163.
89. Welt CK, Carmina E. Clinical review: lifecycle of polycystic ovary syndrome (PCOS): from in utero to menopause. *J Clin Endocrinol Metab*. 2013;**98**(12):4629–4638.
90. Cho YH, Craig ME, Donaghue KC. Puberty as an accelerator for diabetes complications. *Pediatr Diabetes*. 2014;**15**(1):18–26.
91. Goran MI, Ball GDC, Cruz ML. Obesity and risk of type 2 diabetes and cardiovascular disease in children and adolescents. *J Clin Endocrinol Metab*. 2003;**88**(4):1417–1427.
92. Kelly LA, Lane CJ, Weigensberg MJ, Toledo-Corral CM, Goran MI. Pubertal changes of insulin sensitivity, acute insulin response, and β-cell function in overweight Latino youth. *J Pediatr*. 2011; **158**(3):442–446.
93. Alexander J, Chang GQ, Dourmashkin JT, Leibowitz SF. Distinct phenotypes of obesity-prone AKR/J, DBA2J and C57BL/6J mice compared to control strains. *Int J Obes*. 2005;**30**(1): 50–59.
94. West DB, Boozer CN, Moody DL, Atkinson RL. Dietary obesity in nine inbred mouse strains. *Am J Physiol*. 1992;**262**(6 Pt 2): R1025–R1032.
95. Mauvais-Jarvis F. Estrogen and androgen receptors: regulators of fuel homeostasis and emerging targets for diabetes and obesity. *Trends Endocrinol Metab*. 2011;**22**(1):24–33.